A Comparative Study of Two Different Octagonal Structure-Based Split Ring Resonators

Durga Prasad Mishra
Department of Electronics and Communication Engineering,
National Institute of Technology,
Rourkela,
Odisha, India
durgaprasad474@gmail.com

Ishu Goyal
Department of Electronics and Communication Engineering,
National Institute of Technology,
Rourkela,
Odisha, India
theishugoyal@gmail.com

Santanu Kumar Behera
Department of Electronics and Communication Engineering,
National Institute of Technology,
Rourkela,
Odisha, India
skbehera@ieee.org

***Abstract*—Radio Frequency Identification (RFID) Tags market has led to a rise in various sectors and applications due to significant advantages over other wireless communication technologies. Due to the edge of not requiring line-of-sight communication, RFID has acquired the barcode technology market. With RFID, the process of automatic tagging and advanced tracking have been much easier. This paper presents the results of a split ring resonator with split length in different patterns with the octagonal ring structure. The tags in the study can be used for ultra-wideband (UWB) applications with a frequency range of 3-11 GHz. Two different split rings were compared to analyze the encoding (number of bits) and the RCS of the tag. The encoding capacity is found to be increased from 3-bits to 5-bits with the change in the split pattern.**

Keywords—Radio Frequency Identification Tag (RFID), resonators, Split Ring Resonator (SRR), chipless tag.

I. Introduction

The wide use of RFID for wireless communication has made a huge demand in the market for various applications such as scanning, materials tracking, library management, tracking of different movements, and many more [1]. With such a vast billion-dollar market, it is growing at an increasing rate of more than 10% each year [2]. Barcodes have been in great use for many years, but since the introduction of chipless technology in RFID, the advantage of being less price per unit results in the mass deployment of RFID tags at a lower cost than barcodes. RFID tags have also overcome the problem of line-of-sight communication, which was needed in barcodes to establish communication with the reader. The RFID system comprises two parts: the tag or transponder and the other is the reader, also named the interrogator. The exchange of information in the RFID system occurs through the reader and transponder. In the case of chipped technology, the transponder generally consists of electronic circuits for signal processing and establishing a connection. The communication or exchange of information takes place with the help of electromagnetic waves. RFID tags can be classified into two types depending on the power supply requirement: active and passive tags. Active tags require some power supply to turn on and communicate with the reader, whereas passive tags do not require an external supply; instead, they get on with the electromagnetic waves. Passive tags depend on the reader to get the power to turn on. Due to such a power reduction, passive RFID suffers from a low reading range [3]. RFID tags need to be attached to the object's body to detect or track the movement. The reader gets data from the tag, placed in the range of the reader, and processes further to provide data to the database, processor, and middleware. The data with the tags can help the reader interpret in the presentable form with identification of the product, especially in packaging and production units. RFID tags can be used as a sensor to sense changes in physical quantities such as temperature, humidity, stress, etc. Such changes can be sensed through the change in resonance of the tag's response [4].

The two varieties of RFID tags differ by an integrated circuit in the tag, enabling chipped RFID tags to process with the help of the integrated blocks such as signal processing unit, rectifier, modulator, demodulator, etc. Nonetheless, its disadvantages include higher cost, security threats, robustness, and recyclability [2]. Table I provides the brief differences between chipped and chipless RFID tags. A pictured block diagram of working is presented in Fig. 1.

Split-ring resonators have been an excellent choice for multi-bit RFID tags and many other applications such as wireless sensors and the aviation industry. Much work has been done regarding split-ring resonators. In [5], an RFID tag of 19-bits based on a complementary split-ring resonator is proposed, designed on Polyethylene-Terephthalate (PET) substrate. The operating frequency range for this transponder is 0.9 to 2.7 GHz. A structure of a spiral resonator with an operating frequency of 3–7 GHz is presented [9]. L-shaped resonators with a frequency range of 4.5–8.0 GHz are discussed in [10]. The chipless RFID U-Slot multi resonator tag designed in [11] has an encoding capacity of 6-bits (fabricated on a C-MET substrate). There is a discussion of split-ring resonators, square-shaped with the encoding capability of 3-bits, in [12].

In this article, a comparison is made between two patterns of the split in split resonator-based RFID tags. The Section II of the paper presents a brief theory about chipless RFID tags.

Section III provides some essential formulas required for

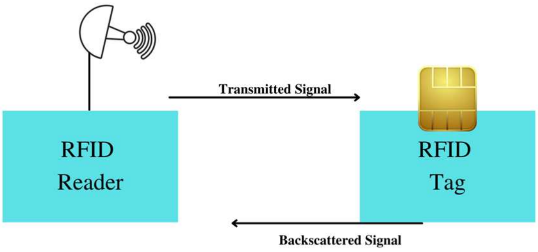

(a) Chipless RFID System

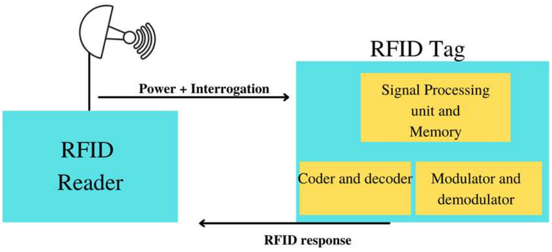

(b) Chipped RFID System

RFID system design. The structure of two transponders are discussed in sections IV and V. A comparative analysis is discussed in section VI. Finally, Section VII presents the conclusion with references at the end.

II. Chipless RFID Tag

Chipless tags comprise mainly three elements, a tag, reader or interrogator, and antenna. It works on the backscattering principle. The tag receives the signal from the reader, which makes it on along with establishing communication. The tag sends back the backscattered signal to the interrogator to transfer the information encoded into the tag. Chipless RFID tags are passive circuits as it doesn't require a battery-powered supply. RFID tags can be designed based on different resonating structures with different shapes. To encode the information from the signal, the reader checks the occurrence of null at resonant frequencies [13].

TABLE I.

Compared Properties of Chipped and Chipless RFID

Ref.	Parameter	Chipped RFID	Chipless RFID
[6]	Cost of tag	Higher as compare to barcodes	Lower from barcodes
[6]	ASIC chip presence	Embedded in the tag	No chip is present
[7]	Average reading distance	5 meters	1 meter
[8]	Noise and interference effects	Low	High due to low power signal
[7]	Frequency range	0.125 MHz to 5.8 GHz	Can be even more than 20 GHz
[8]	Power transmitted	3 to 4 W or more	Less than 10 mW
[8]	Nature	Brittle	Flexible in versatile applications

Fig. 1. Pictorial view of (a) Chipless RFID (b) Conventional Chipped RFID.

III. RFID Design Theory

While designing an RFID transponder, the Radar Cross Section (RCS) is an important variable to consider, which defines the effective area through which the reader receives the required backscattered signal for further application. RCS of the chipped tag can be formulated as in (1) [6].

$$\sigma = \frac{\lambda^2 R_a G_{tag}^2}{\Pi |Z_a + Z_c|} \tag{1}$$

Where λ represents the wavelength associated with the signal with operating frequency, R_a represents the antenna's input impedance Z_a real part, G_{tag} represents the gain of an antenna associated with the tag, and Z_c represents chipped RFID impedance.

The above equation can be changed to chipless RFID tags assuming the match of the antenna to the transmission line of 50 Ω, which gives Z_c = 50 Ω. While taking Z_a = real at the resonant frequency, the above equation can be defined as (2).

$$\sigma = \frac{\lambda^2 R_a G_{tag}^2}{\Pi |2Z_a|} = \frac{\lambda^2 G_{tag}^2}{2\pi} \tag{2}$$

According to the sensitivity of the reader, the maximum read-range for the chipless RFID is given by (3) [6].

$$R_{max} = \frac{\lambda}{4\pi}\sqrt{\frac{P_i P_{PLF} G_r G_t}{P_m}} \tag{3}$$

Where P_i denotes the input power associated with the chipless tag, P_{PLF} denotes polarization loss factor, G_r denotes the reader's gain, G_t denotes the tag's normalized gain, and P_m denotes minimum sensitivity of the reader's receiver.

According to the radar range equation described in [14], the received and transmitted power ratio can be determined for a chipless RFID with the RCS value σ. The ratio can be defined as (4).

$$\frac{P_r}{P_t} = \sigma \frac{G_0^2 \lambda^2}{(4\Pi)^3 R^4} \tag{4}$$

Where G_0 is receiver or transmitter gain and R is the target's distance from the receiver and transmitter antenna.

IV. Design of Transponder 1

The design of transponder 1 is based on the octagonal ring structure, in which six octagonal rings with varying gaps are present [15]. There is also an octagonal solid at the center on the inner side of the structure. The substrate taken for the design is Taconic TLX-8 with the epsilon value of 2.55 and loss tangent value of 0.002. The dimensions of the substrate taken are 26 × 26 × 0.1 mm^3. The splits are created in the octagonal structure, with a 3 to 11 GHz operating frequency range. With this structure, the encoding capacity is 3-bits. The structure is suitable for the UWB applications with 3-bits information. The gap of splits created in each octagonal ring has the dimension of 1 mm. The labeled diagram of the structure of transponder 1 is shown in Fig. 2.

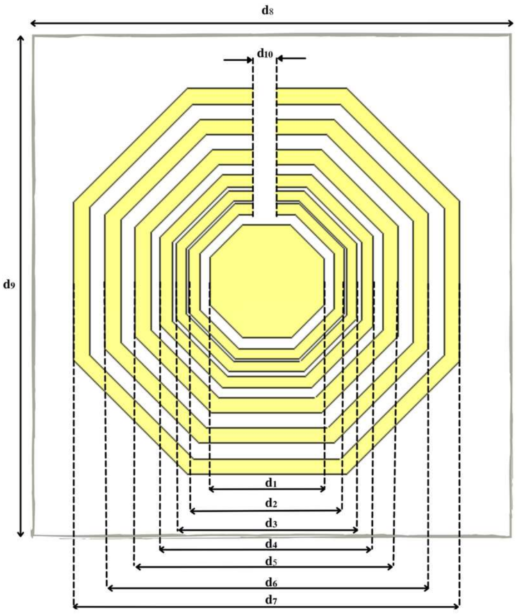

Fig. 2. Structure of transponder 1.

The values of dimensions shown in Fig. 2 are tabulated in Table II. A rectangular patch is used to create a split in the structure. The measurements were selected [15] and analyzed dynamically to get a better RCS response from the structure. The variable 'd_9' is the length and the variable 'd_8' is the width of the substrate. The length 'd_{10}' denotes the dimension of the split gap in the layout figure, as shown in Fig. 2. The variable 'd_1' represents the horizontal width of the inner octagonal structure, and remained variables 'd_2,' 'd_3,' 'd_4', 'd_5,' 'd_6,' and 'd_7' are the horizontal widths of octagonal ring resonators from inner to the outer side.

TABLE II.

Dimensions of Structure

Length	**Value (mm)**
d_1	6.60
d_2	9.00
d_3	10.5
d_4	12.4
d_5	15.3
d_6	18.8
d_7	22.4
d_8	26.0
d_9	26.0
d_{10}	1.00

The tag simulation for RCS is done through the CST Studio Suite 2021 student version. The RCS response at three resonant peaks is shown in Table III. The RCS response is presented in Fig. 3, with three resonant peaks at 6.72 GHz, 8.07 GHz, and 10.04 GHz. The maximum RCS is -22.568 dBsm which is suitable in the UWB applications.

TABLE III.

RCS at Resonant Peaks

Resonant Frequency (GHz)	RCS (dBsm)
6.72	-22.568
8.07	-23.448
10.04	-23.878

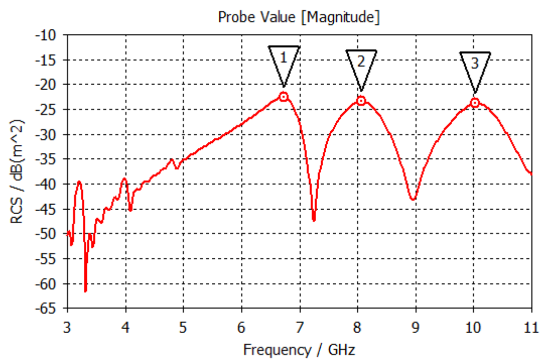

Fig. 3. RCS response curve of transponder 1.

From the simulation, three bits are obtained as suggested by the number of resonating peaks [16] in Fig. 3, which validate the results to the desired number of bits. Fig. 4 presents the surface current distribution for the respective tag. The surface current distribution plot is shown for three distinct frequencies at which the peak occurred.

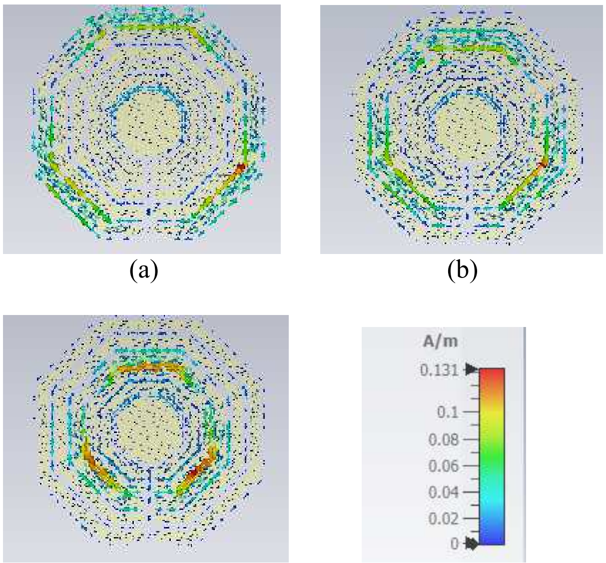

Fig. 4. Current distribution for transponder 1 at (a) 6.72 GHz, (b) 8.07 GHz, and (c) 10.04 GHz.

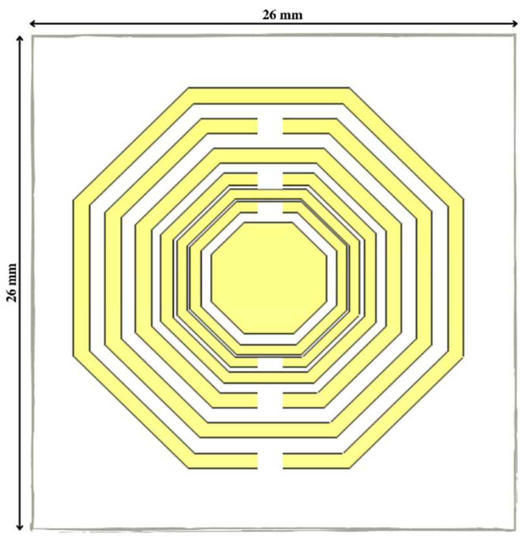

Fig. 5. Structure of transponder 2.

V. DESIGN OF TRANSPONDER 2

The second structure is also based on an octagonal ring structure with six rings and one solid octagon on the inner side. The dimensions of the substrate are the same as transponder 1. Also, the dimensions of the rings and the inner solid are the same as transponder 1. In this structure, the splits in the rings are generated in the fashion shown in Fig. 5. The dimension of the split gap is taken as 1 mm.

Taconic TLX-8 is used as the substrate to design this structure of transponder 2. CST Studio Suite student version 2021 is used to get the RCS curve response. With the change in the split pattern, the bit capacity of the structure turned out to be 5-bits. Five resonant peaks were obtained while simulation, i.e., 3.60 GHz, 4.80 GHz, 6.59 GHz, 8.52 GHz, and 10.25 GHz. The RCS curve for structure 2 is shown in Fig. 6.

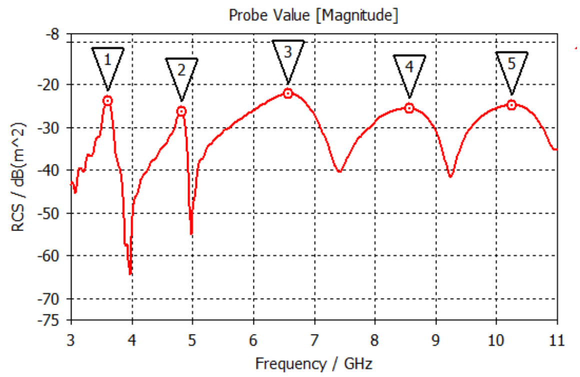

Fig. 6. RCS response curve of transponder 2.

The value of RCS for each resonating structure is given in Table IV. The maximum RCS obtained with the transponder 2 is -22.020 dBsm at 6.59 GHz.

TABLE IV.

RCS AT RESONANT PEAKS

Resonant Frequency (GHz)	RCS (dBsm)
3.60	-23.735
4.80	-26.085
6.59	-22.020
8.52	-25.516
10.25	-24.757

The simulated response (Fig. 6) shows the encoding capacity of 5-bits, which validates the results. For the resonant peaks, the current distribution is shown in Fig. 7.

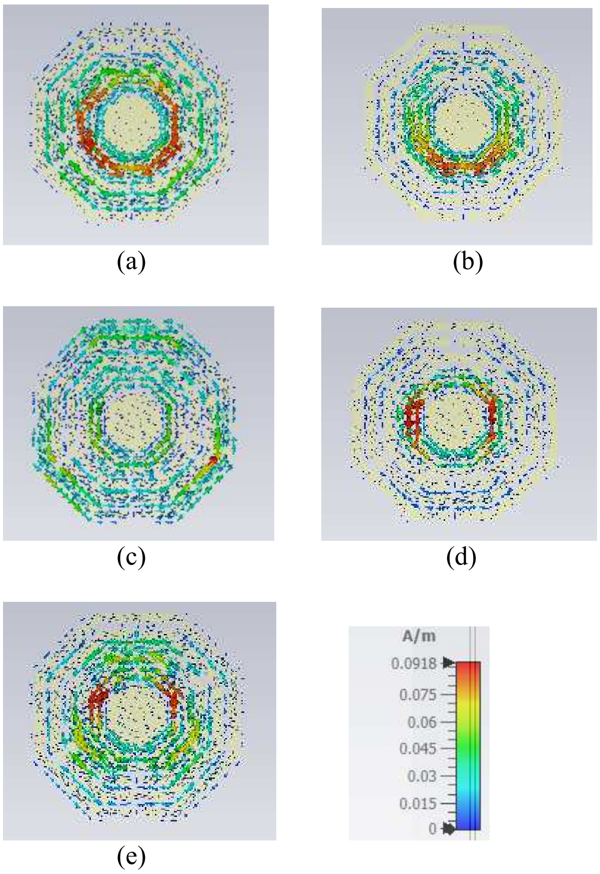

Fig. 7. Current distribution for transponder 2 at (a) 3.60 GHz, (b) 4.80 GHz, (c) 6.59 GHz, (d) 8.52 GHz, and (e) 10.25 GHz.

VI. COMPARATIVE ANALYSIS

Transponders 1 and 2 were designed and analyzed based on different parameters. The proposed two structures have the same structure, substrate, and parameters. The change in the fashion of splitting enhanced the properties of some variables or parameters of RFID design. The encoding capacity of the octagonal structure increased from 3-bits in structure 1 to 5-bits in structure 2; the RCS also improved from -22.568 in structure 1 to -22.020 in structure 2, without changing the size and material of the substrate. With the wide frequency range of both structures, these can be used for UWB applications. A comparative analysis of transponders 1 and 2 with other various proposed designs in different references is shown in Table V. The applications of multiple resonators RFID structures are given in Table VI.

TABLE VI.

APPLICATIONS OF VARIOUS RESONATORS

Ref.	S. No.	RFID Types	Applications
[9]	1	Spiral Ring Resonator	Low-cost item-tagging such as documents which need more security and banknotes
[17]	2	Metallic Strip Resonator	Item tracking and identification
[18]	3	Open Stub Resonator	Efficient contactless data capturing
Proposed Work	4	Octagonal Split Ring Resonators	Retail and biomedical sector, medical imaging

TABLE V. COMPARISON OF VARIOUS PROPOSED TAGS

Sl. No.	Reference	RFID Types	Material	Frequency Range (GHz)	Dimensions	No. of bits	Bits/GHz	ε_r
1	[9]	Spiral Resonator	Taconic TLX-0	3-7	65 × 88 mm^2	35	8.75	2.45
2	[17]	Metallic Strip Resonator	FR-4	2-7	2 × 4 cm^2	23	4.6	4.6
3	[18]	Open Stub Resonator	Substrate with ε_r = 4.4, tan δ = 0.0018	1.5-4.5	50 × 30 mm^2	8	2.67	4.4
4	Proposed design 1	Octagonal Split Ring Resonator (transponder 1)	Taconic TLX-8	3-11	26 × 26 mm^2	3	0.375	2.55
5	Proposed design 2	Octagonal Complementary Split Ring Resonator (transponder 2)	Taconic TLX-8	3-11	26 × 26 mm^2	5	0.625	2.55

VII. CONCLUSION

The research article shows a comparative analysis of two structures based on octagonal structure. With the change in dimension of splits in the structure, the encoding capacity increased, and RCS improved with structure 2. With the five resonators pair, which acts as an LC circuit, the structure 2 RCS encoding capacity of information bits increased to five. The designed structure works with the frequency range of 3 to 11 GHz, which implies wide application in UWB. The plots of current distribution provided an insight into the validation of the structure with the maximum current at the inner ring at the higher resonant frequency and vice-versa.

REFERENCES

[1] D. P. Mishra and S. K. Behera, "Multibit Coded Passive Hybrid Resonator Based RFID Transponder With Windowing Analysis," *IEEE Transactions on Instrumentation and Measurement*, vol. 71, pp. 1-7, 2022, Art no. 8005907, doi: 10.1109/TIM.2022.3201538.

[2] S. Tedjini, N. Karmakar, E. Perret, A. Vena, R. Koswatta, E. Rubayet et al., "Hold the chips: Chipless technology, an alternative technique for RFID," *IEEE Microwave Magazine*, vol. 14, no. 5, pp. 56–65, 2013.

[3] Durga Prasad, et al. "Modified rectangular resonator based 15-bit chipless radio frequency identification transponder for healthcare and retail applications." *International Journal of RF and Microwave Computer-Aided Engineering* 32.6 (2022): e23127.

[4] M. Borgese, F. A. Dicandia, F. Costa, S. Genovesi, and G. Manara, "An Inkjet Printed Chipless RFID Sensor for Wireless Humidity Monitoring," *IEEE Sensors Journal*, vol. 17, no. 15, pp. 4699- 4707, 2017, doi: 10.1109/JSEN.2017.2712190.

[5] M. E. B. Jalil et al., "High Capacity and Miniaturized Flexible Chipless RFID Tag Using Modified Complementary Split Ring Resonator," *IEEE Access*, vol. 9, pp. 33929-33943, 2021, doi: 10.1109/ACCESS.2021.3061792.

[6] N. C. Karmaker, "Tag, You're It Radar Cross Section of Chipless RFID Tags," *IEEE Microwave Magazine*, vol. 17, no. 7, pp. 64-74, July 2016, doi: 10.1109/MMM.2016.2549160.

[7] S. K. Behera and N. C. Karmakar, "Wearable Chipless RadioFrequency Identification Tags for Biomedical Applications: A Review [Antenna Applications Corner]," *IEEE Antennas and Propagation Magazine*, vol. 62, no. 3, pp. 94-104, June 2020, doi: 10.1109/MAP.2020.2983978.

[8] Mishra, Durga Prasad, and Santanu Kumar Behera. "Modified rectangular resonators based multi - frequency narrow - band RFID reader antenna." *Microwave and Optical Technology Letters* 64, no. 3 (2022): 544-551.

[9] S. Preradovic, I. Balbin, N. C. Karmakar, and G. F. Swiegers, "Multiresonator-based chipless RFID system for low-cost item tracking," *IEEE Transactions on Microwave Theory and Techniques*, vol. 57, no. 5, pp. 1411–1419, 2009.

[10] U. A. Haider, M. Noman, H. Ullah and F. A. Tahir, "A Compact L-Shaped 16 Bit Polarization Independent Chipless RFID Tag," 2020 International Conference on UK-China Emerging Technologies (UCET), Glasgow, United Kingdom, 2020, pp. 1-3, doi: 10.1109/UCET51115.2020.9205384.

[11] Sumi M, Dinesh R, Nijas C M, S. Mridula and P. Mohanan, "U slot multi-resonator RFID tag with enhanced bit encoding capacity," 2016 IEEE Region 10 Conference (TENCON), 2016, pp. 116-119, doi: 10.1109/TENCON.2016.7847970.

[12] D. P. Mishra, T. Kumar Das, P. Sethy and S. K. Behera, "Design of a Multi-bit Chipless RFID Tag using Square Split-ring Resonators," *2019 IEEE Indian Conference on Antennas and Propogation (InCAP),* 2019, pp. 1-4, doi: 10.1109/InCAP47789.2019.9134626.

[13] Sumi, M. & Pradeep, Anju & Paul, Binu & Shanta, Mridula. (2017). High Security Chipless RFID Tags Using Frequency Shift Coding Technique. Radioengineering. 26. 765-771. 10.13164/re.2017.0765.

[14] Balanis, Antenna Theory Analysis and Design, 3rd ed. Hoboken, NJ: Wiley, 2005.

[15] D. Betancourt, K. Haase, A. Hübler and F. Ellinger, "Bending and Folding Effect Study of Flexible Fully Printed and Late-Stage Codified Octagonal Chipless RFID Tags," *IEEE Transactions on Antennas and Propagation*, vol. 64, no. 7, pp. 2815-2823, July 2016, doi: 10.1109/TAP.2016.2559522.

[16] Mishra, Durga Prasad, Tanmaya Kumar Das, Santanu Kumar Behera, and Nemai Chandra Karmakar. "Modified rectangular resonator-based 15-bit chipless radio frequency identification transponder for healthcare and retail applications," *International Journal of RF and Microwave Computer-Aided Engineering: e23127, 2022.*

[17] A. Vena, E. Perret, and S. Tedjini, ''Chipless RFID tag using hybrid coding technique,'' *IEEE Transactions on Microwave Theory and Techniques*, vol. 59, no. 12, pp. 3356–3364, Dec. 2011.

[18] C. M. Nijas, R. Dinesh, U. Deepak, A. Rasheed, S. Mridula, K. Vasudevan, and P. Mohanan, ''Chipless RFID tag using multiple microstrip open stub resonators,*'' IEEE Transactions on Antennas and Propagation*, vol. 60, no. 9, pp. 4429–4432, Sep. 2012.